A micellar-enhanced fluorescence photoinduced four-way calibration method for the determination of multiclass pesticides in lemon juice

Marina Antonio, Mirta R. Alcaraz, R. Dario Falcone, María J. Culzoni

PII: S0003-2670(23)00999-6

DOI: https://doi.org/10.1016/j.aca.2023.341778

Reference: ACA 341778

To appear in: *Analytica Chimica Acta*

Received Date: 31 March 2023

Revised Date: 8 August 2023

Accepted Date: 2 September 2023

Please cite this article as: M. Antonio, M.R. Alcaraz, R.D. Falcone, Marí.J. Culzoni, A micellar-enhanced fluorescence photoinduced four-way calibration method for the determination of multiclass pesticides in lemon juice, *Analytica Chimica Acta* (2023), doi: https://doi.org/10.1016/j.aca.2023.341778.

Credit author statement

Marina Antonio: Methodology, Formal analysis, Investigation, Writing - Review & Editing

Mirta Raquel Alcaraz: Conceptualization, Methodology, Writing - Review & Editing

R. Dario Falcone: Conceptualization, Methodology, Writing - Review & Editing

María J. Culzoni: Conceptualization, Methodology, Writing - Review & Editing, Supervision

ACA-23-1036

A micellar-enhanced fluorescence photoinduced four-way calibration method for the determination of multiclass pesticides in lemon juice

Marina Antonio[a,b], Mirta R. Alcaraz[a,b]*, R. Dario Falcone[c,d], María J. Culzoni[a,b]*

[a] *Laboratorio de Desarrollo Analítico y Quimiometría (LADAQ), Facultad de Bioquímica y Ciencias Biológicas, Universidad Nacional del Litoral, Ciudad Universitaria, Santa Fe 3000, Argentina*

[b] *Consejo Nacional de Investigaciones Científicas y Técnicas (CONICET), Godoy Cruz 2290, CABA (C1425FQB), Argentina*

[c] *Departamento de Química, Universidad Nacional de Río Cuarto, Ruta Nacional 36, km 601, Río Cuarto* (*X5804BYA), Córdoba, Argentina*

[d] *Instituto para el Desarrollo Agroindustrial y de la Salud (IDAS, CONICET-UNRC), Ruta Nacional 36, km 601, Río Cuarto* (*X5804BYA), Córdoba, Argentina*

[*] Corresponding authors: malcaraz@fbcb.unl.edu.ar (M.R. Alcaraz) and mculzoni@fbcb.unl.edu.ar (M.J. Culzoni)

Abstract

In this work, a four-way multivariate calibration method for the simultaneous determination of four pesticides - carbendazim (CBZ), thiabendazole (TBZ), pirimiphos-methyl (PMM), and clothianidin (CLT) - in lemon juice is presented. Third-order data were acquired by registering the photoinduced fluorescence of the analytes as excitation-emission matrices at different times of UV-light irradiation, in the presence of organized media (direct micelles) as fluorescence enhancers. The optimal experimental conditions (pH 11.5 and 32 mmol L^{-1} hexadecyltrimethylammonium chloride surfactant) were determined through a central composite design using the response surface methodology. The analytes were individually calibrated, except for TBZ and CBZ due to the inner filter effect of TBZ on CBZ. Test samples containing all analytes and imidacloprid (as potential interference) were analyzed. PARAFAC was utilized to evaluate both the trilinearity and quadrilinearity of the third-order data and four-way arrays, respectively. PMM was successfully determined with quadrilinear PARAFAC decomposition, whereas CLT, TBZ, and CBZ were satisfactorily modelled using U-PLS/RTL due to the loss of quadrilinearity caused by different phenomena. The profitable applicability of the analytical method in the CBZ, TBZ, PMM, and CLT determination in lemon juice samples was demonstrated, achieving limits of detection below the maximum residue levels reported by the European Commission, and mean recoveries at 90±5%.

Keywords: Multiclass pesticides; Photo-reaction; Organized media; Four-way calibration method; Lemon juice

1. Introduction

According to the last report of the Food Agricultural Organization (FAO) [1], Argentina is the second largest producer of citrus in South America and the principal exporter of lemons worldwide. For addressing the high demand, great efforts are continually made to improve the yield and quality of the products, which are constantly threatened by harmful organisms, pests, and plant diseases. In this regard, chemical control has been gaining ground in the agricultural production system because of its high effectiveness in pest and disease control [2].

Pesticides are substances used as herbicides, fungicides, and insecticides, among others, and play a key role in modern agriculture systems since they can prevent, reduce, or eliminate pests. Particularly, in citrus production, combinations of diverse classes of pesticides are employed to enhance their effectiveness and improve yields. However, their application implies that pesticide residues may remain in the fruits, involving possible risks to human health and the ecosystem [3]. The most used pesticides in citrus fruits are organophosphates (OPs), organochlorines (OCs), neonicotinoids, and azoles, which proved to be the major source of soil and water pollution and are capable of causing toxic effects in humans and animals [4–6]. To guarantee the quality and safety of citrus fruits, the European Commission (EC) [7] and the United States Food and Drug Administration (USFDA) [8] established the maximum residue limits (MRLs) of pesticides, defined as the highest level of pesticide residue that is legally tolerated in or on food when pesticides are applied. In Argentina, these limits are defined by the National Food Safety and Quality Service (SENASA) [9].

In the literature, different analytical techniques focused on several pesticide residues determination in citrus fruits at levels of the MRLs are reported. The most employed techniques are gas chromatography-tandem mass spectrometry (GC-MS/MS) [10] and high-performance liquid chromatography (HPLC) coupled with diode array (DAD) [11], fluorescence [12] and MS detectors [13]. Despite their high sensitivity and selectivity, the low concentration of

pesticide residues found in these complex samples requires several sample treatments and enrichment processes to enhance the performance of the analytical method, which demand the use of organic solvents and are time-consuming.

In pursuing the development of efficient, simple, fast, and sustainable analytical methodologies, spectroscopy emerges as a promising alternative. In this regard, fluorescence-based methodologies have proved to be compelling approaches that guarantee high sensitivity and selectivity with a dramatic reduction in organic solvent consumption [14]. In addition, the formulation of organized media by self-assembly of compounds such as amphiphilic cyclodextrins or surfactants can induce or enhance the fluorescence emission of certain compounds [15,16], leveraging the performance of the analytical method due to improvements in sensitivity and detection capabilities.

For many years, multivariate calibration-based techniques have been attracting the attention of researchers in several fields, since they proved to be a good approach that aids in enhancing the proficiency of analytical methods through the use of mathematical procedures, entailing a significant reduction in the experimental work, in agreement with the principles and fundamentals of the green analytical chemistry (GAC) [17]. In particular, second and higher-order calibration methods have the capability of accurately detecting several components, even in the presence of interferences or unexpected components. This property is called "second-order advantage" and it has been widely exploited in the direction of bettering the performance of the analyses.

In the present work, the development of an optimized micellar-enhanced fluorescence photoinduced four-way calibration method for the simultaneous determination of four multiclass pesticides commonly used in lemons is presented. The data were acquired by registering the photoinduced fluorescence of the analytes as excitation-emission matrices (EEM) at different times of UV-light irradiation, in the presence of organized media (direct

micelles) as a fluorescence enhancer. The quadrilinearity property of the four-way data was evaluated with PARAFAC and the results were discussed. The four-way arrays with loss of quadrilinearity were analysed in depth and the proper algorithms for modelling were chosen to exploit the intrinsic properties of the data.

2. Materials and methods

2.1. Chemicals and reagents

All standards were of analytical grade. Pirimiphos methyl (PMM, 99.3 %), clothianidin (CLT, 99.9 %), thiabendazole (TBZ, ≥ 99 %), carbendazim (CBZ, ≥ 98 %), imidacloprid (IMD, ≥ 98 %), polyoxyethylene (23) lauryl ether (Brij-35, ≥ 90 %), sodium dodecylbenzene sulfonate (SDBS, 98 %) and hexadecyl trimethyl ammonium chloride (HTAC, 98 %) were provided by Sigma-Aldrich (St. Louis, MO, USA). LC-grade methanol (MeOH) and acetonitrile (ACN) were obtained from Merck (Darmstadt, Germany). Sodium hydroxide (NaOH), monobasic sodium phosphate (NaH_2PO_4), anhydrous magnesium sulfate ($MgSO_4$), and sodium chloride (NaCl), all of analytical grade, were purchased from Biopack (Buenos Aires, Argentina). Primary secondary amine (PSA) and activated carbon (C_{act}) were supplied from Phenomenex (Torrance, CA, USA) and Ciccarelli (Buenos Aires, Argentina), respectively. Ultrapure water was obtained from a Milli-Q water purification system from Millipore (Bedford, MA, USA).

2.2. Solutions and standard samples

PMM, TBZ, and CBZ stock solutions were prepared by dissolution of the appropriate amounts of each pesticide in MeOH, while CLT and IMD standard solutions were prepared in ACN. Stock solution concentrations were *ca.* 500 mg L^{-1} for PMM and CBZ, and *ca.* 1000.0 mg L^{-1} for TBZ, CLT, and IMD. All the solutions were maintained at 4°C in the dark for four months. Working standard solutions of *ca.* 50.0 mg L^{-1} were daily prepared by

transferring the proper aliquots of the pesticide stock solutions to 1.0 mL volumetric flasks and completing the mark with MeOH or ACN, as appropriate.

Phosphate buffer solution (NaPS) 0.01 mol L^{-1} was prepared by dissolution of the appropriate amounts of NaH_2PO_4 in ultrapure water. pH was adjusted between 8.0–11.5 with NaOH, as appropriate. 250 mmol L^{-1} Brij-35, 150 mmol L^{-1} SDBS, and 200 mmol L^{-1} HTAC solutions were daily prepared by dissolving the appropriate amount of the powder in ultrapure water.

2.3. Calibration and test samples

5-level concentration sample sets of pure PMM and CLT standards were prepared in triplicate by transferring the appropriate aliquot of the corresponding working solution and 160 µL of the HTAC solution to 1.0 mL volumetric flasks and completing the mark with NaPS pH 11.5. The final pesticide concentrations ranged between 30 – 150 µg L^{-1} and 500 – 1700 µg L^{-1} for PMM and CLT, respectively.

Since TBZ has an inner filter effect on CBZ fluorescence, a calibration set of 20 mixed solutions containing TBZ and CBZ was randomly prepared in 5 concentration levels by transferring the appropriate aliquots of each working solution and 160 µL of the HTAC solution to 1.0 mL volumetric flasks, and completing the mark with NaPS pH 11.5. The final pesticide concentrations ranged between 30 – 110 µg L^{-1} and 40 – 200 µg L^{-1} for TBZ and CBZ, respectively.

A 16-sample test set was built by mixing the four pesticides at concentrations different than those used to calibrate, by following a random design. IMD was incorporated in these samples as non-modelled interferent at different concentrations, as detailed in Table 2. The test samples were prepared as previously described for the calibration samples.

147 *2.4. Lemon samples*

148 All lemon fruits were directly obtained from lemon trees without pesticide treatment.
149 After arrival at the laboratory, the fruits were immediately washed with Milli-Q water and
150 stored at 4 °C for no more than 5 days until all assays were performed. To obtain a homogenized
151 sample of fresh lemon juice, 6 randomly selected fruits were cut into two pieces, and the juice
152 was mechanically extracted. The juice was maintained at 4 ºC for up to 3 days, if necessary.

153 Aliquots of lemon juice were spiked with PMM, CLT, CBZ, and TBZ following the same
154 random design employed to prepare the test sample set, to build a spiked sample set.
155 Appropriate aliquots of each working solution were transferred to 5.0 mL of fresh lemon juice.
156 The samples were then properly homogenized using a vortex mixer and maintained at room
157 temperature in the dark for 2 hours before analysis.

158

159 *2.5. QuEChERS-based procedure*

160 The sample pre-treatment was performed employing a quick, easy, cheap, effective,
161 rugged, and safe extraction (QuEChERS)-based methodology, schematically depicted in Fig.
162 1.

163 In a glass centrifuge tube containing 5.0 mL of blank or spiked lemon juice sample, as
164 appropriate, 5.0 mL of ACN was added, and the mixture was mechanically shaken with a vortex
165 for 1 min to guarantee homogeneity. Then, 2.0 g of anhydrous $MgSO_4$ and 0.5 g of NaCl were
166 added and the tube was mechanically shaken with a vortex for 1 min and centrifuged for 10 min
167 at 3000 rpm to allow phase separation. For the clean-up step, 4.0 mL of supernatant (SN, the
168 organic phase) was transferred into a glass centrifuge tube, and 150 mg of PSA, 450 mg of
169 anhydrous $MgSO_4$, and 200 mg of C_{act} were added to remove the matrix pigments. The mixture
170 was mechanically shaken with a vortex for 1 min, subjected to ultrasound for 10 min, and
171 centrifuged for 15 min at 3000 rpm. The SN was then transferred to a Khan tube and dried

under a gentle stream of nitrogen at 40 g°C using a nitrogen evaporator. The final residue was reconstituted with 160 µL of HTAC solution and completed to 1.0 mL with NaPS 0.01 mol L^{-1} pH 11.5.

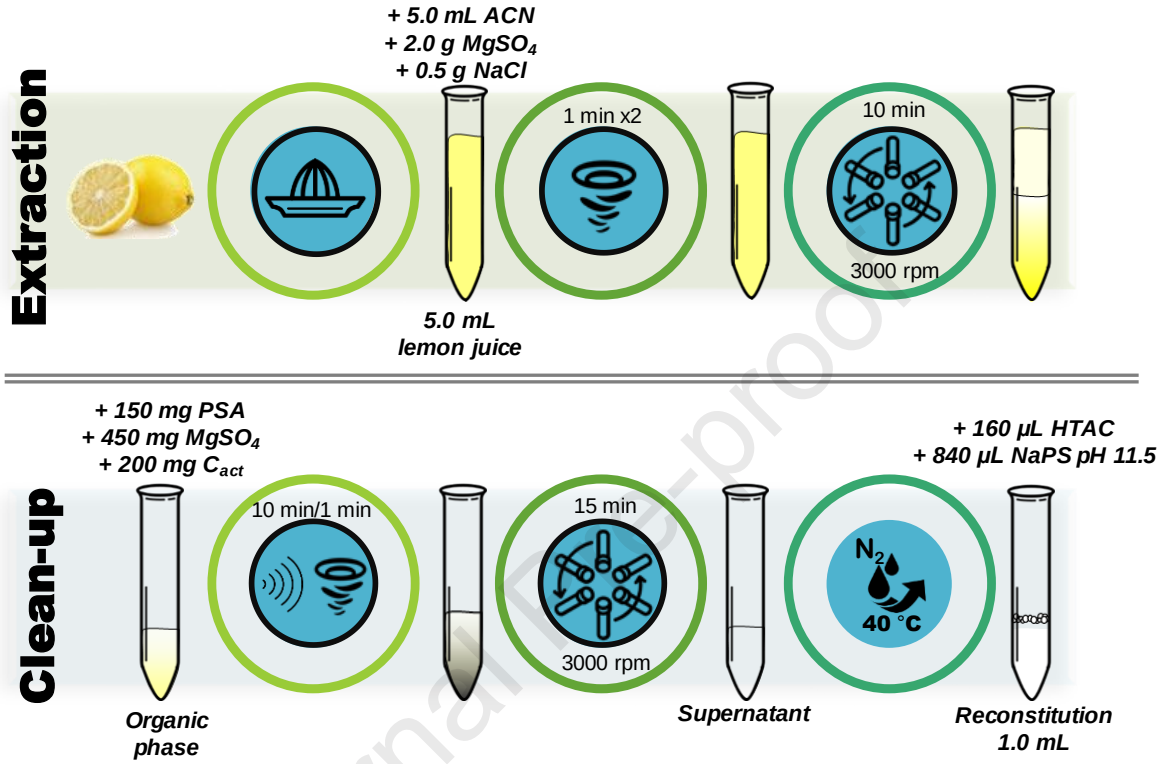

Figure 1. Schematic illustration of the (QuEChERS)-based methodology employed for sample pre-treatment.

2.6. Optimization of the photochemical reaction conditions

In light of the difference in nature between the analytes, and considering that the photochemical reaction efficiency depends on several experimental variables, the response surface methodology (RSM) with a central composite design (CCD) was used to derive the optimal conditions of the photochemical reaction with a reduced number of experiments.

After a preliminary analysis, the factors selected for the optimization were the NaPS pH of the HTAC concentration. A total of 21 experiments were generated by the CCD (Table S1) and they were randomly performed to guarantee the independence of the results. In all

experiments, the concentrations of the analytes remained constant at a level of 100 μg L^{-1} CBZ, 80 μg L^{-1} TBZ, 50 μg L^{-1} PMM, and 500 μg L^{-1} CLT.

The third-order data acquired for each CCD experiment was individually subjected to PARAFAC decomposition, and the photochemical reaction time and the fluorescence contribution of each analyte were obtained as responses. After response modelling, the optimization was accomplished by using the desirability function [18].

2.7. Instrumental procedure and data generation

The spectrofluorometric measurements were performed on a Cary Eclipse fluorescence spectrophotometer (Agilent Technologies, Waldbronn, Germany) equipped with a xenon flash lamp, using a quartz-cell of 10×2 mm optical path length. 254 nm-UV light irradiation was performed using the pulsed xenon light source of the spectrophotometer.

The EEMs were recorded covering the excitation range of 245–380 nm, every 5 nm, and the emission range of 300–440 nm, every 3 nm, using a scan rate of 7200 nm min^{-1}, a PMT voltage of 650 V, and excitation and emission slits of 10 nm. All experiments were performed at room temperature.

Third-order data were generated by measuring the EEMs at different periods of UV-light irradiation, completing a total of 360 s/240 s (before/after optimization) irradiation, every 30 s. Hence, the three-dimensional arrays obtained before the optimization comprised 13×28×48 datapoints for irradiation time, excitation, and emission dimensions, respectively. After the optimization, the data were of 9×28×48 length for irradiation time, excitation, and emission dimensions, respectively.

2.8. Software

The Cary Eclipse Package software (Agilent Technologies, Waldbronn, Germany) was employed for instrument control and data acquisition. Experimental design, surface response modelling, and desirability function calculations were performed using Stat-Ease Design-Expert 8.0.0 (Stat-Ease, Inc., Minneapolis, USA) [19].

All chemometric models were implemented in MATLAB R2015a (The MathWorks Inc., Massachusetts, USA, 2015) [20]. PARAFAC, *A*PARAFAC, and U-PLS/RTL were implemented by using the MVC3 toolbox for MATLAB R2015a, which is freely available at www.iquir-conicet.gov.ar/descargas/mvc3.rar [21]. Rayleigh and Raman scatterings were removed using the *EEM_corr* MATLAB GUI, available at https://fbcb.web1.unl.edu.ar/laboratorios/ladaq/download/ [22].

3. Results and discussion

3.1. General considerations

For chemometric-based applications, a comprehensive evaluation of the underlying data properties promotes the development of multi-way calibration methods with the greatest likelihood of success. For instance, multilinearity is one of the most important data features that drive the selection of the algorithm for data modelling. In third-order data analysis, multilinearity is expressed in terms of trilinearity. Furthermore, when a sample set is analysed, the three-dimensional arrays of each sample can be organized into a four-way object, and quadrilinearity must be evaluated [23]. The relationship between concentration and the analytical signal will also motivate the election of some algorithms over others.

In the present case, the analytical methodology consists of registering EEM at the end of a photochemical reaction triggered by UV-light irradiation, which generates changes in the fluorescent signal while it is applied, but not in its absence. Hence, the EEMs are acquired at

steady-state conditions. In this regard, the third-order data obtained for a single sample comprised the photochemical reaction behaviour, the excitation, and the emission wavelength dimensions, and fulfilled the criterion of trilinearity. When several samples are jointly analysed and full synchronization and independence between modes are observed, the data fulfil the criterion of quadrilinearity. Otherwise, some issues in the four-way data object break the quadrilinearity [24]. For instance, in kinetics, some reactions depend on the initial concentration of the analytes, provoking a lack of reproducibility in the photo-reaction profile between samples, which entails nonquadrilinearity type 1 data generation. Quadrilinearity can also be affected by the inner filter effect, a phenomenon that causes variations in the excitation and emission spectra of the analyte in the presence of some sample constituents [25]. When the inner filter effect simultaneously occurs in the excitation and emission modes, nonquadrilinearity type 2 arises [23].

PARAFAC is a widespread algorithm that performs multilinear decomposition of multidimensional data (three or more dimensions). The most important characteristic of this algorithm is that the solutions are often unique, in addition to the ability to provide meaningful profiles [26]. In this regard, trilinear third-order data or quadrilinear four-way arrays can be properly subjected to PARAFAC, obtaining profiles that can be comprehensively analysed for quantitative or qualitative purposes. These characteristics make PARAFAC suitable for multilinearity evaluation aiding in characterizing the data and selecting the proper algorithm for the modelling [26,27]. In this work, PARAFAC was applied to evaluate the trilinearity fulfilment of the individual third-order data (photochemical reaction-EEM) and the quadrilinearity of the four-way arrays.

3.2. Optimization of the experimental conditions

3.2.1. Preliminary studies

Pesticides as organophosphates and chlorinated hydrocarbons, among others, undergo hydrolysis promoting their decomposition in aqueous solutions at a pH higher than 7 [28]. Therefore, the higher the pH, the faster the pesticide decomposition or degradation by hydrolysis [29]. Preliminary studies showed that the photochemical reaction of pesticides in aqueous solutions at different pHs (5-12), adjusted with HCl and NaOH, does not arouse observable changes in the fluorescent signals of the analytes after 6 minutes of UV-light irradiation (data not shown). Notwithstanding, changes in the fluorescent signal at pH >8 were noticed when NaPS was used instead of NaOH to control the pH, either as an enhancement/detriment of the native intensity or as the arising of a new fluorescent band, which can be attributed to the degradation of the pesticides.

On the other hand, it has been proved that the organized media presence not only provokes a sensitivity enhancement in some fluorescence-based determinations but also improves the selectivity by displacement of the analyte emission bands concerning aqueous conditions [16,30]. Thus, to improve the figures of merit of the method, the influence of cationic (HTAC), anionic (SDBS), and non-ionic (Brij-35) surfactants on the photoinduced fluorescence signal of the pesticide was evaluated in NaPS solutions. In all cases, they were added at the beginning of the reaction, as a constituent of the background solution, at levels above the critical micellar concentration. For CBZ, TBZ, and PMM, HTAC was the surfactant that significantly enhanced the native fluorescence intensity concerning that observed in the absence of surfactant (Fig. S1). Moreover, it was proved that HTAC enhances the fluorescence intensity of the photochemical product of CLT, which does not have an observable native fluorescence signal.

3.2.2. Data acquisition and analysis

Considering the preliminary results, a CCD approach was performed to establish the best combination of factors, i.e., pH (8.0–11.5) and HTAC concentration (10–60 mmol L^{-1}), that ensures the effectiveness of the photochemical reaction in terms of reaction rate and analyte micellar-enhanced fluorescence intensity (MEFI).

For each experiment, trilinear third-order data comprising excitation, emission, and photochemical reaction time modes was acquired and subjected to PARAFAC decomposition to gather the CCD responses. In all cases, the core consistency (CORCONDIA) and the lack of fit (LOF) of the modelling were considered to determine the number of spectroscopically active components [26]. For PARAFAC modelling, initial estimates by random initialization were used, and the non-negativity constraint was applied to the three modes. The decomposition results rendered approximations to pure constituent profiles, such as the spectral and kinetic profiles shown in Fig. 2, which were then used to obtain the CCD responses.

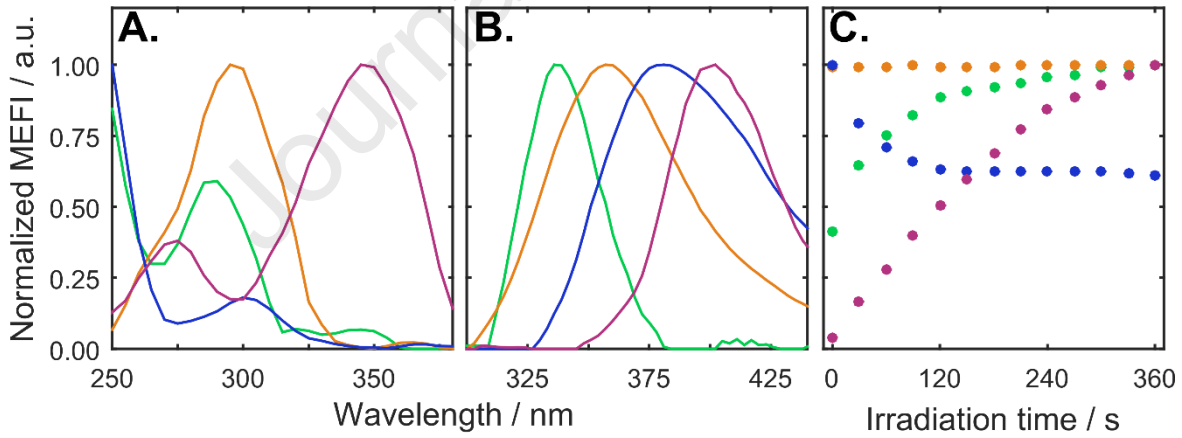

Figure 2. (**A**) Excitation, (**B**) emission, and (**C**) photochemical reaction profiles of CBZ (green), TBZ (orange), PMM (blue), and CLT (pink) obtained by PARAFAC modelling of the CCD experiment Nº 12 data.

As can be appreciated, CBZ and CLT present weak and null native fluorescence, respectively, which increases as the photochemical reaction evolves. This behaviour suggests

the generation of fluorescent products as a consequence of their photochemical degradation. A different trend is observed for PMM, for which the strong native fluorescence decays along with the irradiation time suggesting the breakdown of the molecules, and for TBZ, whose fluorescence remained stable.

Some of the CCD responses were obtained through curve-fitting procedures of the photochemical PARAFAC profiles. As can be appreciated in Fig. 3A, CBZ, and CLT follow a kinetic growth behaviour, which could be adequately described by a sigmoid Boltzmann function, as follows:

$$y = A_2 + \frac{(A_1 - A_2)}{1 + exp^{\frac{(x-x_0)}{dx}}} \quad (1)$$

where y is the MEFI, x is the irradiation time, x_0 is the centre of the curve, and A_1 and A_2 are the upper and lower MEFI limits. dx represents the time interval in which the abrupt change in the MEFI occurs. In these reactions, the CCD response was the time at which the reaction reaches the equilibrium or plateau (Tp). The parameter was obtained from the fitted Boltzmann function as the tangent to the curve passing through its centre (x_0), according to the procedure described by Aguiar et al. [31], following Eq.2:

$$Tp = x_0 + 2dx \quad (2)$$

Contrarily, PMM follows a behaviour that could be properly fitted using a single exponential decay function (Fig. 3B), according to Eq.3:

$$y = y_0 + A \times \exp\left(-\frac{x}{t}\right) \quad (3)$$

where y is the MEFI, y_0 is the native MEFI, x is the irradiation time, and A is the lower limit of MEFI. t is the reaction rate obtained from the slope of the decay curve.

Last, the maximum MEFIs of TBZ, CBZ, and CLT were taken at the end of the irradiation procedure, while for PMM, the maximum MEFI value was considered as the native fluorescence signal, i.e., the intensity before the UV-light irradiation.

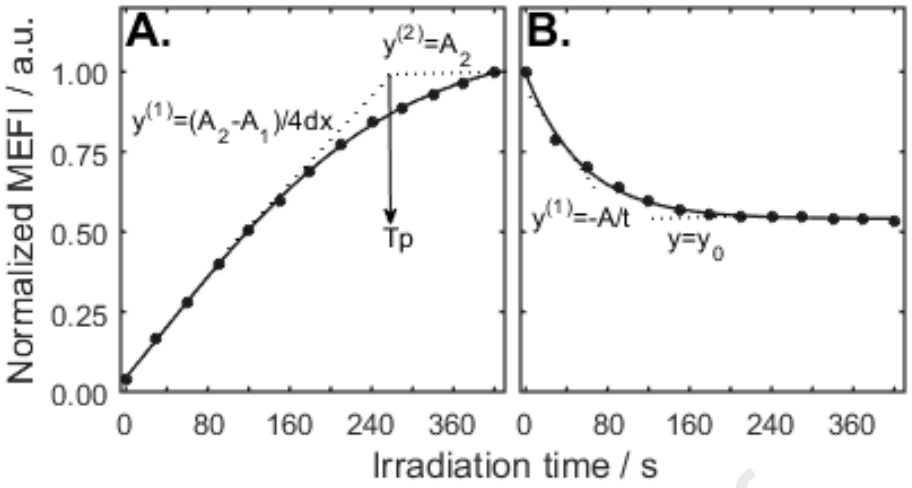

Figure 3. (**A**) Typical photochemical profile of CBZ and CLT with growing Boltzmann-type fitting for *Tp* estimation. (**B**) Typical photochemical profile of PMM with exponential decay fitting for *t* estimation.

In conclusion, the 7 responses obtained from the experiments and used in the optimization procedure were TBZ, CBZ, and CLT MEFI at 360 s; native PMM MEFI; CLT and CBZ *Tp*; and PMM *t*. All the responses are summarized in Table S1.

3.2.3. Central composite design optimization

An ANOVA test with backward selection, at a significance level of 0.05, was implemented to find the model that best fits the relation between each response and the experimental factors. Table 1 summarizes the ANOVA results indicating the significance of the experimental factors in each model, the associated probability values (*p*) for model significance and LOF, and the adjusted correlation coefficients (R^2).

The results indicate that all responses follow cubic models and suggest that both pH and HTAC concentration significantly affect the MEFI of all analytes, the PMM *t*, and the CLT *Tp* (Fig. S2). However, the one obtained for CBZ *Tp* showed no significance, suggesting

independence between the response and the experimental factors. Hence, this response was not included in the subsequent optimization stage.

Then, the simultaneous optimization of the experimental conditions was carried out by using the desirability function (also known as Derringer, *D*) [18]. *D* values range from 0 to 1, referring to the null and fully desirable solutions, respectively. As can be seen in Table S2 different criteria were followed to simultaneously optimize the six responses. For instance, the concentration of HTAC was minimized to reduce the interferences and dispersions caused by the medium, whereas the MEFI was maximized to improve the analytical figures of merit (AFOMs) of the methodology. Moreover, the preferred level of PMM *t* and CLT *Tp* was the minimum as they refer to the time required to finish the reaction since, as can be appreciated in Fig. 3, the higher the CLT *Tp* value, the slower the reaction (Fig. 3A), whereas the higher the PMM *t* value, the faster the reaction (Fig. 3B).

The values yielded by the *D* function (*D*=0.593) suggest that the optimal experimental conditions are reached when using an HTAC concentration of 31.66 mmol L^{-1} and a medium pH of 11.5. To minimize operational errors in the preparation of the solutions, the concentration of HTAC was fixed at 32 mmol L^{-1}. Fig. S3 shows the surface of the *D* results according to the pH and the HTAC concentration.

Subsequently, the predicted conditions were experimentally verified in triplicate (Table S3), and the reliability of the model was evaluated by employing a *t*-test. Considering a level of α=0.05, the t_{exp} values were lower than the critical $t_{(\alpha,\upsilon)}$ for all responses, indicating that there were no statistically significant differences between the responses at a confident level of 95%, proving the accuracy of the mathematical models and the reliability of the results. Thus, the calibration method development was accomplished by utilizing the optimal experimental conditions of 32 mmol L^{-1} HTAC at pH 11.5 with a total irradiation time of 240 s.

Table 1. Model fitting of the responses obtained from the CCD

Response		Model [a]	ANOVA results		R^2 *pred.*	R^2 *Adj.*	CV (%) [c]
			p-value [b]	Lack of fit			
MEFI	CBZ	A, B, AB, A^2, B^2, A^2B, AB^2	< 0.0001	0.9726	0.9852	0.9917	2.04
	TBZ	A, B, A^2, B^2, AB^2	< 0.0001	0.2619	0.9847	0.9892	2.28
	PMM	A, B, A^2, B^2, AB^2	< 0.0001	0.5657	0.8518	0.9144	4.54
	CLT	A, B, A^2, B^2, AB^2	< 0.0001	0.1277	0.9007	0.9453	2.59
Reaction time	t_{PMM}	B, A^2, A^3	0.0002	0.5892	0.5049	0.6661	6.16
	Tp_{CLT}	A, B, A^2, B^2, A^2B, AB^2	< 0.0001	0.6448	0.9369	0.9535	10.01

[a] Factors studied: A: pH, B: HTAC concentration (mmol L^{-1})
[b] Terms were considered significant with *p*-values < 0.05
[c] CV: coefficient of variation

Last, the PARAFAC spectral profiles obtained at the optimal conditions ($\mathbf{s_1}$) were benchmarked against the real profiles of the analytes ($\mathbf{s_2}$) to quantitatively evaluate the reliability of the decomposition. At this point, it should be clarified that the spectral comparison of CBZ and TBZ was done by utilizing the PARAFAC profiles obtained after the decomposition of the data corresponding to a binary mixture as a reference ($\mathbf{s_2}$) because of the spectral distortion of the CBZ by the inner filter effect of TBZ. The spectral comparison was performed by using the criterion of spectral overlapping degree s_{12}, (Pearson's correlation coefficient) estimated as [32]:

$$s_{12} = \frac{\|\mathbf{s_1^T s_2}\|}{\|\mathbf{s_1}\|\|\mathbf{s_2}\|} \quad (4)$$

The value s_{12} ranges from 0 to 1, corresponding to no overlapping and full overlapping, respectively. The retrieved s_{12} values for excitation/emission spectra of PMM, CLT, CBZ, and TBZ were 0.99910/0.99598, 0.99771/0.99987, 0.99909/0.99816, and 0.98553/0.99981, respectively. These figures allow us to ascertain the good quality of the PARAFAC decomposition and, hence, the reliability of the modelling.

3.3. Four-way calibration method development

3.3.1. Data processing considerations

First, it is worth mentioning that three sets of calibration samples were prepared with the aim of exploiting the intrinsic properties of the data according to the behaviour of the analytes in the presence of the sample constituents. CLT and PMM were individually calibrated and the photochemical behaviour at different concentrations was thoroughly analyzed. For this purpose, individual third-order data obtained for different analyte concentrations were subjected to trilinear PARAFAC decomposition, and the retrieved profiles were benchmarked against each other. For PARAFAC modelling, initial estimates by random initialization were used, and the non-negativity constraint was applied to the four modes. This analysis aided to unravel a perfect overlapping of the PMM profiles (Fig. 4A), and a concentration-dependency in the CLT photochemical behaviour (Fig. 4B). This evidence allows us to conclude that the concentration mode of the CLT four-way data is a quadrilinearity breaking mode and, in consequence, nonquadrilinear type 1 data is acquired [23] and also asserts the fact that the PMM four-way data fulfil the criterion of quadrilinearity, which was then corroborated with further predictive analyses.

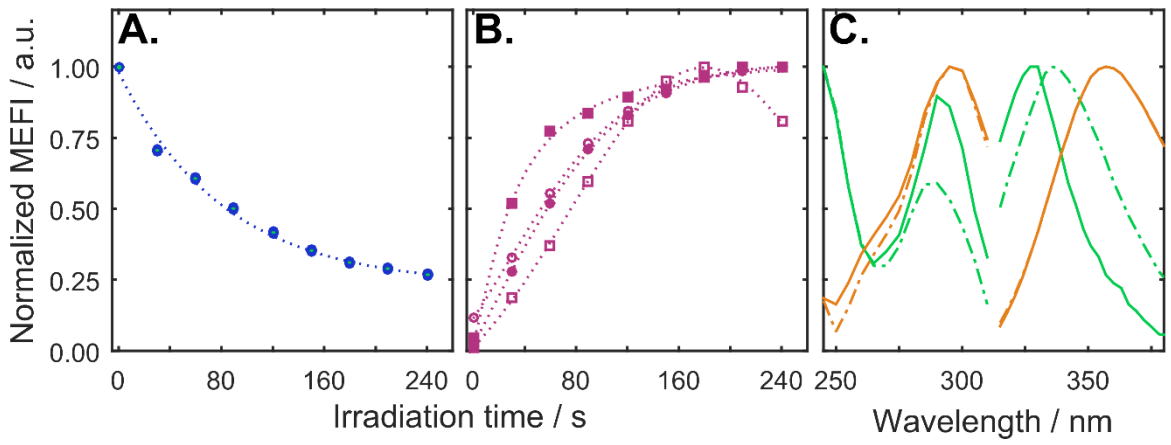

Figure 4. (**A**) Photochemical reaction profiles of 30 μg L^{-1} (●) and 150 μg L^{-1} (○) solutions of PMM obtained from PARAFAC. (**B**) Photochemical reaction profiles of 500 μg L^{-1} (●), 1700

μg L^{-1} (○), 2000 μg L^{-1} (■) and 3000 μg L^{-1} (□) solutions of CLT obtained from PARAFAC. (**C**) CBZ (green) excitation and emission spectra in the presence (dashed line) and absence (solid line) of TBZ (orange).

On the other hand, binary samples were built for TBZ and CBZ calibration because of the inner filter effect of TBZ on the CBZ fluorescence. In general terms, this phenomenon arises when one or several sample constituents absorb radiation from that emitted by the analyte, and it is evidenced as an analyte spectral distortion, which depends on the presence and concentration of the compound responsible for the inner filter effect [25]. In the present case, the TBZ spectra remain invariant against variations in the CBZ concentration while CBZ spectra are seriously affected by the presence and changes in the concentration of TBZ. From the chemometric standpoint, this effect leads to a break in the quadrilinear structure of the four-way data. Since both emission and excitation spectra of CBZ vary from sample to sample as a consequence of the inner filter effect, two modes of the four-way structure are considered quadrilinearity-breaking modes (Fig. 4C). Hence, according to the classification data structure reported by Olivieri and Escandar [33], nonquadrilinear type 2 data is obtained. To demonstrate this observation, a four-way data array, built with the calibration and test samples, was subjected to quadrilinear PARAFAC decomposition, and the results were evaluated in terms of recovery and reproducibility. The predictive figures rendered for TBZ were rather satisfactory (REP%= 9.1 %), whereas the predicted CBZ concentrations were significantly different from the nominal values (REP%= 110 %), proving the lack of quadrilinearity of the four-way data.

All these considerations aided in finding the best calibration model for each analyte capitalizing on the intrinsic characteristic of the data and the individual particularities of the chemometric algorithms.

3.3.2. Data modelling and quantitative analysis

Relying on the fact that four-way data built for PMM samples fulfil the criterion of quadrilinearity, the calibration method was built by applying quadrilinear PARAFAC decomposition. In this regard, a four-way data array was built with the third-order data of the 15 calibration samples and one test sample and was then subjected to decomposition. For the chemometric modelling, initial estimates by random initialization were used, and non-negativity constraint in the four modes was applied in the ALS optimization. To determine the number of spectroscopically active components, the core consistency (CORCONDIA) and the LOF of the modelling were considered. It is worth mentioning that the number of components was always in accordance with the real number of the sample constituents. To quantitatively evaluate the reliability of the decomposition, the spectral comparison between the PARAFAC profile and real spectra was carried out by obtaining the s_{12} estimator, according to Eq. 4. The values s_{12} for excitation/emission spectra of PMM were 0.99687/0.99943, shedding light on the good performance of the decomposition.

For CLT, it was proved that the four-way data array is nonquadrilinear type 1 due to the lack of reproducibility in the photochemical reaction profile along the concentration mode. Under this scenario, and capitalizing on the fact that the third-order data of the calibration and test samples fulfil the criterion of trilinearity, two chemometric approaches were evaluated. The first approach consisted of the implementation of the augmented PARAFAC (*A*PARAFAC) model to an augmented trilinear three-way data array. The second approach involved the decomposition through a latent-structured methodology, considering the linear relationship between the concentration of the analyte and the MEFI. Thus, unfolded PLS with residual trilinearization (U-PLS/RTL) was used.

*A*PARAFAC is an algorithm that exploits the ability to bear nonquadrilinear type 1 data utilizing the augmentation strategy but preserving the original three-dimensional structure of

the data [34]. For the modelling, third-order data corresponding to different samples was appended on each other in a way that guarantees the trilinearity of the augmented object, i.e., an array augmented along the photochemical reaction mode. To initiate the decomposition, initial estimates by random initialization were used and non-negativity constraint in the four modes was applied in the ALS optimization.

On the other hand, U-PLS/RTL presents the capability to deal with a slight loss of quadrilinearity, albeit trilinearity of the residuals must be assured [35]. For the modelling, the number of calibration latent variables (LV) was determined using the leave-one-out cross-validation method described by Haaland and Thomas [36]. The number of LV was set at six, considering the background and emitting constituents generated during the CLT photochemical reaction. The estimation of the proper number of RTL was based on the evaluation of the residuals obtained when a different number of RTL was utilized, in terms of residual fit and loading features. When using three RTL components in test samples decomposition, the retrieved residual profiles demonstrated that the third one featured the noise structure, reaching a good stabilization of the residuals. Therefore, three RTL were used. The predictive figures (REP= 10.1 %) revealed that even though *A*PARAFAC retains the original structure of the data, aiding in reaching unicity in the results, U-PLS/RTL rendered better predictive figures since its intrinsic flexibility leverages the predictive performance of the method.

Finally, in the case of TBZ/CBZ, U-PLS/RTL was implemented since it has been widely proven that this algorithm can successfully cope with nonquadrilinear type 2 data [25]. The number of LV in the test sample was set at five for TBZ and six for CBZ, using two or three RTL components, as appropriate.

The predictive results obtained for the four analytes in the test samples, in the presence of IMD as a potential interferent, are summarized in Table 2. As can be seen, the relative errors of prediction (REP%) are below 6.4% in all cases proving the excellent predictive capability of

476 the developed method. Moreover, to appraise whether the recoveries are statistically different
477 that 100% or not, a hypothesis test was conducted. For this, an experimental *t* value was
478 estimated for each calibration model, as follows:

$$t_{exp} = |100 - \bar{R}| \frac{\sqrt{I}}{SR} \quad (5)$$

479 where $\bar{R}$ is the mean experimental recovery, *SR* is the standard deviation of the recoveries and
480 *I* is the number of samples. The recoveries are considered statistically different than 100% when
481 t_{exp} exceeds the critical $t_{(\alpha,\upsilon)}$ value at level α and υ=*I*-1 degree of freedom [37]. Here, considering
482 a level of α=0.05, the t_{exp} values were lower than the critical $t_{(0.05,15)}$ =2.13 for all analytes,
483 indicating that the experimental recoveries are not statistically different from 100%, and
484 therefore asserting the accuracy of the method.

485

Table 2. Predicted concentrations of PMM, CLT, TBZ, and CBZ in test samples containing IMD as a potential interferent.

Sample	Analyte[a]							
	PMM[b]		CLT[c]		TBZ[d]		CBZ[d]	
	Nominal	Predicted [e]	Nominal	Predicted [e]	Nominal	Predicted [e]	Nominal	Predicted [e]
V1	45.0	43.5 (96.7)	650	696 (107)	40.0	40.0 (100)	60.0	66.0 (110)
V2	75.0	69.9 (93.1)	950	930 (98.3)	60.0	60.8 (102)	100.0	108.0 (108)
V3	105.0	108.0 (103)	1250	1250 (100)	80.0	75.0 (93.8)	140.0	140.0 (100)
V4	135.0	134.0 (99.3)	1550	1520 (98.1)	100.0	102.0 (102)	180.0	182.0 (101)
REP% [f]	6.4		4.9		6.2		5.9	
Mean recovery ($\bar{R}$%)	97.7		101		99.4		102	
t_{exp} [g]	1.44		0.32		0.44		1.32	

[a] Concentrations are expressed in μg mL^{-1}
[b] Quadrilinear four-way data modelled with PARAFAC
[c] Nonquadrilinear type 1 four-way data modelled with U-PLS/RTL
[d] Nonquadrilinear type 2 four-way data modelled with U-PLS/RTL
[e] Between parenthesis, the mean recovery of the quadruplicate expressed in %
[f] Relative Error of Prediction in %, $REP\% = 100 \times \sqrt{\frac{1}{I}\sum_{I}^{1}(c_{nom} - c_{pred})^2}/\bar{c}$; where *I* is the number of validation samples; c_{nom} and c_{pred} are the nominal and predicted concentration, respectively; and $\bar{c}$ is the mean calibration concentration
[g] Experimental *t* value, $t_{exp} = |100 - \bar{R}| \frac{\sqrt{I}}{SR}$, where SR is the standard deviation of the recoveries.

486

To graphically illustrate the predictive ability of the developed methods, the elliptical joint of confidence region test (EJCR) was performed. The elliptical domains obtained for all analytes contain the theoretically expected point (1,0) for slope and intercept, respectively, indicating the accuracy of the proposed methodologies (Fig. 5).

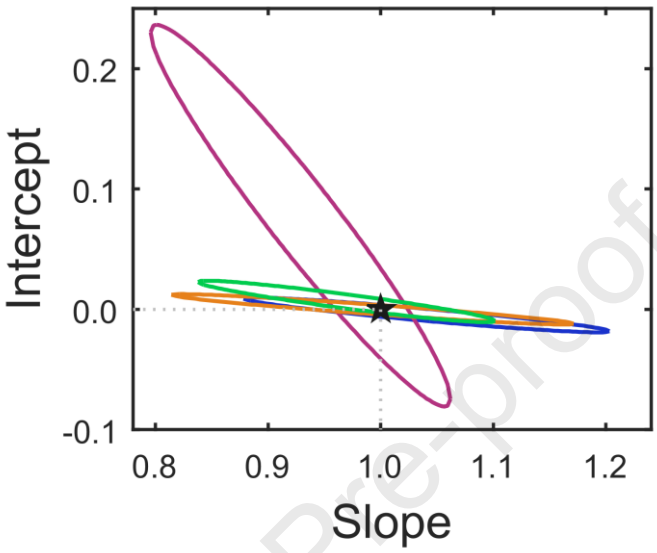

Figure 5. EJCR plots for CBZ (green), TBZ (orange), PMM (blue), and CLT (pink) obtained for test samples.

3.3.3. Real samples analysis

To assess the ability of the developed analytical method to determine the pesticides in real samples, a predictive analysis of the four pesticides in lemon juice samples was carried out. It should be mentioned that the sample treatment methodology allowed for reaching a pre-concentration factor of 5. Hence, lemon juice samples were spiked with the pesticides at concentration levels 5 times lower than those used in the test samples.

Despite the implementation of an exhaustive cleaning procedure, some sample constituents remained in the measured solution. These constituents showed fluorescence signals that overlap the signal of the analytes and, therefore, should be considered during the chemometric analysis. For instance, the number of components used in the PMM PARAFAC

505 analysis was seven, higher than the one used to model the test samples. Likewise, the modelling
506 of CLT, TBZ, and CBZ through U-PLS/RTL involved a higher number of RTL. In addition,
507 blank lemon juice samples, i.e., not spiked, were analysed.

508 Table 3 resumes the predicted concentrations of PMM, CLT, CBZ, and TBZ in spiked
509 and blank lemon juice samples. It can be noticed that the mean recoveries of the four analytes
510 were ranging from 84% to 94% with REP% oscillating between 10 and 18%. All these figures
511 prove the feasibility of the method to determine pesticides at very low concentration levels,
512 even in the presence of highly complex samples, with satisfactory results.

513

Table 3. Predicted concentrations of PMM, CLT, TBZ, and CBZ in the blank and spiked lemon juice samples containing IMD as a potential interferent.

Sample	Analyte[a]							
	PMM[b]		CLT[c]		TBZ[d]		CBZ[d]	
	Nominal	Predicted [e]	Nominal	Predicted [e]	Nominal	Predicted [e]	Nominal	Predicted [e]
R0	-	ND	-	ND	-	ND	-	ND
R1	9.0	7.4(82.5)	130	102 (77.9)	8.0	7.7 (96.7)	12.0	11.2 (93.3)
R2	15.0	12.7 (84.3)	190	166 (87.4)	12.0	10.8 (90.0)	20.0	19.5 (97.5)
R3	21.0	17.9 (81.4)	250	219 (87.8)	16.0	14.9 (93.3)	28.0	25.7 (91.6)
R4	27.0	23.2 (85.7)	310	285 (92.1)	20.0	17.0 (84.8)	36.0	32.7 (93.1)
REP% [f]	17.8		14.1		10.6		12.0	
Mean recovery ($\bar{R}$%)	84.5		86.5		92.2		93.5	

[a] Concentrations are expressed in μg L^{-1}
[b] Quadrilinear four-way data modelled with PARAFAC
[c] Nonquadrilinear type 1 four-way data modelled with U-PLS/RTL
[d] Nonquadrilinear type 2 four-way data modelled with U-PLS/RTL
[e] Between parenthesis, the mean recovery of the quadruplicate expressed in %
[f] Relative Error of Prediction in %, $REP\% = 100 \times \sqrt{\frac{1}{I}\sum_{I}^{1}\left(c_{nom} - c_{pred}\right)^2}/\bar{c}$; where I is the number of validation samples; c_{nom} and c_{pred} are the nominal and predicted concentration, respectively; and $\bar{c}$ is the mean calibration concentration

514 As can be observed, PMM analysis entails the poorest analytical figures in comparison
515 to the other analytes. This effect can be a consequence of the sample treatment procedure since
516 one of the sorbents utilized in the clean-up stage (activated carbon) is also used for the remotion
517 of PMM in contaminated water [38], albeit it acts as an efficient cleaning agent in samples that
518 are highly pigmented [39]. Nevertheless, it was utilized pursuing a reduction in the general

519 cost of the method, considering that the cost of active carbon is considerably less than other
520 carbon-based sorbents, such as graphitized carbon black.
521
522 *3.3.4. Analytical figures of merit*
523 AFOMs are numerical parameters that aid in comprehensively describing the performance
524 of the analytical methodology in terms of detection and prediction capabilities. When
525 estimating AFOMs, a compelling issue that should be considered in advance is the order of the
526 data, as well as the algorithm that was used for its analysis, to obtain representative figures of
527 the method [37].
528 Sensitivity (SEN) is one of the most important AFOMs and can be defined as the variation
529 in the net response for a given variation in the analyte concentration. Limit of detection (LOD)
530 and quantitation (LOQ) are outstanding figures directly related to SEN. Given the fact that SEN
531 is a sample-dependent parameter, LOD (and LOQ) also depends on the sample since the
532 detection of an analyte may vary between samples of different compositions [40]. Hence, the
533 LOD and LOQ of each pesticide were estimated for test and real samples according to ref [40].
534

Table 4. Analytical figures of merit in test and lemon juice samples.

AFOMs	Analyte[a]							
	PMM[b]		CLT[c]		TBZ[d]		CBZ[d]	
	Test	Juice	Test	Juice	Test	Juice	Test	Juice
SEN [a]	28.9	24.3	0.5	0.34	$5.8\ 10^{-3}$	$3.3\ 10^{-3}$	$3.8\ 10^{-3}$	$2.7\ 10^{-3}$
$[\gamma^{-1}]$ [b]	$2.7\ 10^{-4}$	$3.5\ 10^{-4}$	0.02	0.04	$1.2\ 10^{-4}$	$3.0\ 10^{-4}$	$1.8\ 10^{-4}$	$3.4\ 10^{-4}$
LOD [c]	17.0	19.0 (3.8) [e]	77.5	151.0 (30.2) [e]	5.7	14.0 (2.8) [e]	11.1	25.5 (5.1) [e]
LOQ [d]	38.5	44.9 (8.9) [e]	234.8	447.6 (89.5) [e]	17.3	42.4 (8.5) [e]	33.6	77.3 (15.5) [e]

[a] Sensitivity, expressed in AUF L μg $^{-1}$, (AUF=arbitrary unity of fluorescence), estimated according to ref [40]
[b] Inverse of analytical sensitivity, expressed in μg L^{-1} AUF^{-1}, (AUF=arbitrary unity of fluorescence), estimated according to ref [40]
[c] Limit of detection expressed in μg L^{-1}, estimated according to ref [40]
[d] Limit of quantitation expressed μg L^{-1}, estimated according to ref [40]
[e] LOD and LOQ considering a preconcentration factor of 5

535
536 As can be seen in Table 4, the LODs obtained for CLT, TBZ, and CBZ in lemon juice are
537 higher than those obtained in test samples, whereas similar figures were obtained for PMM.

This phenomenon can be explained as a slight detriment in the selectivity of the method due to the presence of sample constituents that emit in the same spectral range. In addition, despite the LODs and LOQs achieved in this work might be rather higher than those reported using HPLC-MS/MS and GC-MS, among others [41,42], the developed method allows determining concentrations below the MRL established by the EU in lemon fruits (MRL_{PMM}=10 µg kg^{-1}; MRL_{CLT}=60 µg kg^{-1}; MRL_{TBZ}=7000 µg kg^{-1}; and MRL_{CBZ}=700 µg kg^{-1}, considering 0.975 kg L^{-1} lemon juice), which reinforce the satisfactory performance of the developed analytical method.

3.4. Analytical greenness evaluation

To quantitatively evaluate the sustainability of the method following the criteria of the GAC, the previously introduced Analytical GREEnness (AGREE) metric approach was implemented [43]. This approach, based on the 12 principles of GAC, retrieves a score between 0 and 1 that comprehensively represents the greenness of the method (the higher the score the greener the method).

In the case of the proposed method, the AGREE metric approach assigned the lowest scores for the sample treatment, sample amount, automation, and solvent toxicity items. The pretreatment of the lemon juice sample allowed the adequate removal of certain fluorescent components that interfered with the quantitation of the analytes. Even though it was not possible to completely avoid the extraction and clean-up steps, minimum amounts of organic solvent (ACN) and non-polluting cleaning agents (PSA and C_{act}) were used, and the whole procedure involved a reduced number of steps. Despite these considerations, the retrieved score of 0.72 endorses the sustainability of the method developed to determine highly environmentally harmful compounds. Figure 6 shows a pictogram depicting the resulting global score and the

performance of the individual criterion on a colour scale which goes from red to green as the numerical value goes from 0 to 1, respectively.

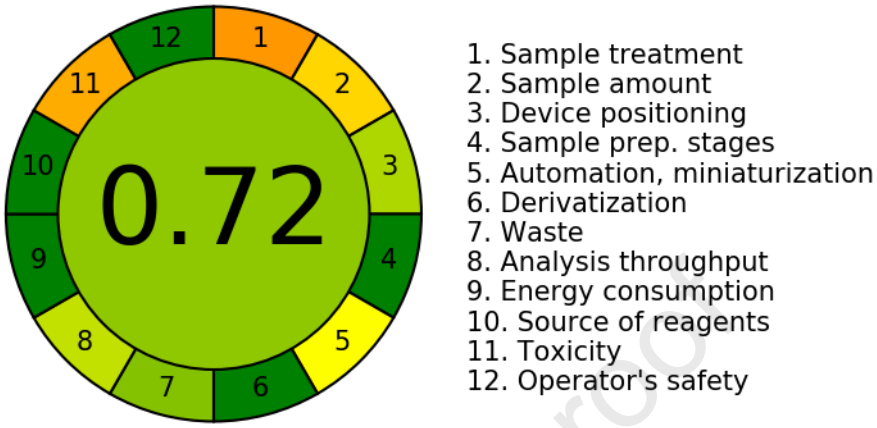

Figure 6. Green assessment of the four-way calibration method developed to determine CBZ, TBZ, PMM and CLT in lemon juice using the AGREE metric software.

4. Conclusions

The combination of a micellar-enhanced fluorescence photoinduced methodology and four-way calibration models empowered the successful determination of four pesticides in lemon juice samples. The optimized photochemical reaction of the analytes has been demonstrated to be a great alternative to reaching a high sensitivity for those analytes with weak fluorescence, as well as an efficient way to enhance the selectivity of the method.

A preliminary evaluation carried out to gain more insight into the chemical behaviour of the analytes against different experimental conditions aided in achieving the optimized conditions that empowered the photochemical reaction in the direction of bettering the performance of the calibration method. Moreover, the intrinsic characteristics of the third-order data were thoroughly investigated to accurately select the chemometric algorithm for data modelling. It has been proved that TBZ has an inner filter effect on CBZ fluorescence which was successfully overcome by designing a proper calibration procedure and selecting U-

582 PLS/RTL for data decomposition. The results show that the CLT photochemical behaviour
583 depends on its concentration, leading to a nonquadrilinear data type 1 that could be conveniently
584 modelled with U-PLS/RTL. Last, a quadrilinear PARAFAC-based method allowed the
585 adequate quantitation of PMM. In light of the results, it can be concluded that the proposed
586 method is highly suitable for the quantitation of pesticides in lemon juice samples in a fast,
587 efficient, and sustainable way.
588

589 **Acknowledgements**

590 We thank Universidad Nacional del Litoral (Project CAI+D 2020-50620190100020LI) and
591 Agencia Nacional de Promoción Científica y Tecnológica (Project PICT 2020-00105) for
592 financial support. M.R.A., R.D.F. and M.J.C. hold a research position at CONICET. MA is a
593 postdoctoral fellow at CONICET.
594

595 **Conflicts of interest**

596 The authors declare that they have no conflict of interest.
597

598 **References**

599 [1] Food and Agriculture Organization, Citrus Fruit Statistical Compendium 2020, Rome,
600 2021. https://www.fao.org/markets-and-trade/commodities/citrus/en/.
601 [2] M. Tudi, H. Daniel Ruan, L. Wang, J. Lyu, R. Sadler, D. Connell, C. Chu, D.T. Phung,
602 Agriculture Development, Pesticide Application and Its Impact on the Environment.,
603 Int. J. Environ. Res. Public Health. 18 (2021). doi:10.3390/ijerph18031112.
604 [3] M.A. Islam, S.M.N. Amin, M.A. Rahman, A.S. Juraimi, M.K. Uddin, C.L. Brown, A.
605 Arshad, Chronic effects of organic pesticides on the aquatic environment and human
606 health: A review, Environ. Nanotechnology, Monit. Manag. 18 (2022) 100740.

doi:https://doi.org/10.1016/j.enmm.2022.100740.

[4] H. Mali, C. Shah, B.H. Raghunandan, A.S. Prajapati, D.H. Patel, U. Trivedi, R.B. Subramanian, Organophosphate pesticides an emerging environmental contaminant: Pollution, toxicity, bioremediation progress, and remaining challenges, J. Environ. Sci. 127 (2023) 234–250. doi:https://doi.org/10.1016/j.jes.2022.04.023.

[5] L. Herbertsson, B.K. Klatt, M. Blasi, M. Rundlöf, H.G. Smith, Seed-coating of rapeseed (Brassica napus) with the neonicotinoid clothianidin affects behaviour of red mason bees (Osmia bicornis) and pollination of strawberry flowers (Fragaria × ananassa)., PLoS One. 17 (2022) e0273851. doi:10.1371/journal.pone.0273851.

[6] M. Ladaniya, Chapter 16 - Postharvest disease management with fungicides, in: M.B.T.-C.F. (Second E. Ladaniya (Ed.), Academic Press, 2023: pp. 563–594. doi:https://doi.org/10.1016/B978-0-323-99306-7.00005-0.

[7] EU, European Commision pesticide MLRs-Regulation (EC) No. 396/2005, (2020). https://ec.europa.eu/food/plant/pesticides/eu-pesticides-database/mrls/?event=search.pr.

[8] United States Food and Drug Administration, Pesticide Residue Monitoring Program Fiscal Year 2020 Pesticide Report, 2022. https://www.fda.gov/food/pesticides/pesticide-residue-monitoring-report-and-data-fy-2020.

[9] Dirección Nacional de Agroquímicos, Productos Veterinarios y Alimentos del Senasa − Resolución-934-2010, (n.d.). http://www.senasa.gov.ar/normativas/.

[10] J.-X. Li, X.-Y. Li, Q.-Y. Chang, Y. Li, L.-H. Jin, G.-F. Pang, C.-L. Fan, Screening of 439 Pesticide Residues in Fruits and Vegetables by Gas Chromatography-Quadrupole-Time-of-Flight Mass Spectrometry Based on TOF Accurate Mass Database and Q-TOF Spectrum Library, J. AOAC Int. 101 (2018) 1631–1638. doi:10.5740/jaoacint.17-0105.

[11] C.A.S. Aguiar Júnior, A.L.R. dos Santos, A.M. de Faria, Disposable pipette extraction

using a selective sorbent for carbendazim residues in orange juice, Food Chem. 309 (2020) 125756. doi:https://doi.org/10.1016/j.foodchem.2019.125756.

[12] O. Hazer, M. Akkbik, D. Demir, Y. Turhan, Determination of carbendazim and chlorpyrifos in selected fruits and vegetables samples using QuEChERS-HPLC-FD, Eurasian J. Anal. Chem. 12 (2017) 17–30. doi:10.12973/ejac.2017.00151a.

[13] E. Calvaruso, G. Cammilleri, A. Pulvirenti, G.M. Lo Dico, G. Lo Cascio, V. Giaccone, V. Vitale Badaco, V. Ciprì, M.M. Alessandra, A. Vella, A. Macaluso, C. Di Bella, V. Ferrantelli, Residues of 165 pesticides in citrus fruits using LC-MS/MS: a study of the pesticides distribution from the peel to the pulp., Nat. Prod. Res. 34 (2020) 34–38. doi:10.1080/14786419.2018.1561682.

[14] E. Sikorska, I. Khmelinskii, M. Sikorski, 19 - Fluorescence spectroscopy and imaging instruments for food quality evaluation, in: J. Zhong, X.B.T.-E.T. for F.Q. Wang (Eds.), Woodhead Publ. Ser. Food Sci. Technol. Nutr., Woodhead Publishing, 2019: pp. 491–533. doi:https://doi.org/10.1016/B978-0-12-814217-2.00019-6.

[15] M. Lezcano, W. Al-Soufi, M. Novo, E. Rodríguez-Núñez, J.V. Tato, Complexation of Several Benzimidazole-Type Fungicides with α- and β-Cyclodextrins, J. Agric. Food Chem. 50 (2002) 108–112. doi:10.1021/jf010927y.

[16] M. Montemurro, R. Brasca, M.J. Culzoni, H.C. Goicoechea, High-performance organized media-enhanced spectrofluorimetric determination of pirimiphos-methyl in maize, Food Chem. 278 (2019) 711–719. doi:https://doi.org/10.1016/j.foodchem.2018.11.090.

[17] H.-L. Wu, T. Wang, R.-Q. Yu, Recent advances in chemical multi-way calibration with second-order or higher-order advantages: Multilinear models, algorithms, related issues and applications, TrAC Trends Anal. Chem. 130 (2020) 115954. doi:https://doi.org/10.1016/j.trac.2020.115954.

[18] G. Derringer, R. Suich, Simultaneous Optimization of Several Response Variables, J. Qual. Technol. 12 (1980) 214–219. doi:10.1080/00224065.1980.11980968.

[19] Design Expert, Stat-Ease Inc., (2010).

[20] S.J. Mazivila, S.A. Bortolato, A.C. Olivieri, MVC3_GUI: A MATLAB graphical user interface for third-order multivariate calibration. An upgrade including new multi-way models, Chemom. Intell. Lab. Syst. 173 (2018) 21–29. doi:https://doi.org/10.1016/j.chemolab.2017.12.012.

[21] A.C. Olivieri, H.-L. Wu, R.-Q. Yu, MVC3: A MATLAB graphical interface toolbox for third-order multivariate calibration, Chemom. Intell. Lab. Syst. 116 (2012) 9–16. doi:https://doi.org/10.1016/j.chemolab.2012.03.018.

[22] F.A. Chiappini, M.R. Alcaraz, H.C. Goicoechea, A.C. Olivieri, A graphical user interface as a new tool for scattering correction in fluorescence data, Chemom. Intell. Lab. Syst. 193 (2019) 103810. doi:https://doi.org/10.1016/j.chemolab.2019.07.009.

[23] A.C. Olivieri, G.M. Escandar, Chapter 11 - Third-order/Four-way Calibration and Beyond, in: A.C. Olivieri, G.M.B.T.-P.T.-W.C. Escandar (Eds.), Elsevier, Boston, 2014: pp. 217–232. doi:https://doi.org/10.1016/B978-0-12-410408-2.00011-9.

[24] M.R. Alcaraz, O. Monago-Maraña, H.C. Goicoechea, A. Muñoz de la Peña, Four- and five-way excitation-emission luminescence-based data acquisition and modeling for analytical applications. A review, Anal. Chim. Acta. 1083 (2019) 41–57. doi:10.1016/j.aca.2019.06.059.

[25] G.N. Piccirilli, G.M. Escandar, Partial least-squares with residual bilinearization for the spectrofluorimetric determination of pesticides. A solution of the problems of inner-filter effects and matrix interferents., Analyst. 131 (2006) 1012–1020. doi:10.1039/b603823a.

[26] R. Bro, PARAFAC. Tutorial and applications, Chemom. Intell. Lab. Syst. 38 (1997)

149–171. doi:https://doi.org/10.1016/S0169-7439(97)00032-4.

[27] C.M. Andersen, R. Bro, Practical aspects of PARAFAC modeling of fluorescence excitation-emission data, J. Chemom. 17 (2003) 200–215. doi:10.1002/cem.790.

[28] E. Dyguda-Kazimierowicz, S. Roszak, W.A. Sokalski, Alkaline Hydrolysis of Organophosphorus Pesticides: The Dependence of the Reaction Mechanism on the Incoming Group Conformation, J. Phys. Chem. B. 118 (2014) 7277–7289. doi:10.1021/jp503382j.

[29] INTERAGRO, High pH can cause alkaline hydrolysis – pesticide breakdown., (n.d.). https://www.interagro.co.uk/high-ph-can-cause-pesticide-breakdown/ (accessed March 28, 2023).

[30] N.A. Alarfaj, M.F. El-Tohamy, Applications of micelle enhancement in luminescence-based analysis, Luminescence. 30 (2015) 3–11. doi:https://doi.org/10.1002/bio.2694.

[31] J. Aguiar, P. Carpena, J.A. Molina-Bolívar, C. Carnero Ruiz, On the determination of the critical micelle concentration by the pyrene 1:3 ratio method, J. Colloid Interface Sci. 258 (2003) 116–122. doi:https://doi.org/10.1016/S0021-9797(02)00082-6.

[32] M.J. Culzoni, H.C. Goicoechea, G.A. Ibañez, V.A. Lozano, N.R. Marsili, A.C. Olivieri, A.P. Pagani, Second-order advantage from kinetic-spectroscopic data matrices in the presence of extreme spectral overlapping: A multivariate curve resolution—Alternating least-squares approach, Anal. Chim. Acta. 614 (2008) 46–57. doi:https://doi.org/10.1016/j.aca.2008.03.013.

[33] A. Olivieri, G. Escandar, Third-order/Four-way Calibration and Beyond, in: 2014: pp. 217–232. doi:10.1016/B978-0-12-410408-2.00011-9.

[34] S.A. Bortolato, V.A. Lozano, A.M. de la Peña, A.C. Olivieri, Novel augmented parallel factor model for four-way calibration of high-performance liquid chromatography–fluorescence excitation–emission data, Chemom. Intell. Lab. Syst. 141 (2015) 1–11.

707 doi:https://doi.org/10.1016/j.chemolab.2014.11.013.
708 [35] A.C. Olivieri, G.M. Escandar, Practical Three-Way Calibration, Elsevier, Waltham,
709 USA, 2014.
710 [36] D.M. Haaland, E. V Thomas, Partial least-squares methods for spectral analyses. 1.
711 Relation to other quantitative calibration methods and the extraction of qualitative
712 information, Anal. Chem. 60 (1988) 1193–1202. doi:10.1021/ac00162a020.
713 [37] A.C. Olivieri, Practical guidelines for reporting results in single- and multi-component
714 analytical calibration: A tutorial, Anal. Chim. Acta. 868 (2015) 10–22.
715 doi:https://doi.org/10.1016/j.aca.2015.01.017.
716 [38] X. Liu, H. Zhang, Y. Ma, X. Wu, L. Meng, Y. Guo, G. Yu, Y. Liu, Graphene-coated
717 silica as a highly efficient sorbent for residual organophosphorus pesticides in water, J.
718 Mater. Chem. A. 1 (2013) 1875–1884. doi:10.1039/C2TA00173J.
719 [39] R.K. Ghosh, S. Majumder, A. Bhattacharyya, A. Paul, Z. Khan, D.P. Ray, S.N.
720 Chattopadhyay, A. Pardeshi, D.B. Shakyawar, K. Banerjee, Introducing a low-cost jute
721 activated carbon as a novel cleanup agent in multiclass pesticide residue analysis using
722 gas chromatography tandem mass spectrometry, J. Clean. Prod. 319 (2021) 128696.
723 doi:https://doi.org/10.1016/j.jclepro.2021.128696.
724 [40] A.C. Olivieri, Analytical Figures of Merit: From Univariate to Multiway Calibration,
725 Chem. Rev. 114 (2014) 5358–5378. doi:10.1021/cr400455s.
726 [41] L. Wu, Y. Song, M. Hu, H. Zhang, A. Yu, C. Yu, Q. Ma, Z. Wang, Application of
727 magnetic solvent bar liquid-phase microextraction for determination of
728 organophosphorus pesticides in fruit juice samples by gas chromatography mass
729 spectrometry, Food Chem. 176 (2015) 197–204.
730 doi:https://doi.org/10.1016/j.foodchem.2014.12.055.
731 [42] Z. Liu, W. Li, X. Zhu, R. Hua, X. Wu, J. Xue, Combination of polyurethane and

polymethyl methacrylate thin films as a microextraction sorbent for rapid adsorption and sensitive determination of neonicotinoid insecticides in fruit juice and tea by ultra high performance liquid chromatography with tand, J. Chromatogr. A. 1659 (2021) 462646. doi:https://doi.org/10.1016/j.chroma.2021.462646.

[43] F. Pena-Pereira, W. Wojnowski, M. Tobiszewski, AGREE—Analytical GREEnness Metric Approach and Software, Anal. Chem. 92 (2020) 10076–10082. doi:10.1021/acs.analchem.0c01887.

- Simultaneous determination of four pesticides in lemon juice by four-way multivariate calibration
- Acquisition of third-order photoinduced fluorescence data
- Use of organized media (direct micelles) as a fluorescence enhancer
- Optimization of the experimental conditions through design of experiments
- Data modeling by means of PARAFAC and U-PLS/RTL

Declaration of interests

☒ The authors declare that they have no known competing financial interests or personal relationships that could have appeared to influence the work reported in this paper.

☐ The authors declare the following financial interests/personal relationships which may be considered as potential competing interests: